haematologica
Journal of the Ferrata Storti Foundation

Common ancestral origin of indeterminate dendritic cell tumor and chronic myelomonocytic leukemia in clonal hematopoiesis

by Aki Sato, Nozomi Yusa, Hiroyuki Takamori, Eigo Shimizu, Koji Jimbo, Seiko Kato, Takaaki Konuma, Kazuaki Yokoyama, Seiya Imoto, Satoshi Takahashi and Yasuhito Nannya

Received: August 18, 2025.
Accepted: December 30, 2025.

Citation: Aki Sato, Nozomi Yusa, Hiroyuki Takamori, Eigo Shimizu, Koji Jimbo, Seiko Kato, Takaaki Konuma, Kazuaki Yokoyama, Seiya Imoto, Satoshi Takahashi and Yasuhito Nannya. Common ancestral origin of indeterminate dendritic cell tumor and chronic myelomonocytic leukemia in clonal hematopoiesis. Haematologica. 2026 Jan 15. doi: 10.3324/haematol.2025.288974 [Epub ahead of print]

CASE REPORTS

Common ancestral origin of indeterminate dendritic cell tumor and chronic myelomonocytic leukemia in clonal hematopoiesis

Aki Sato,[1*] Nozomi Yusa,[2] Hiroyuki Takamori,[3,4] Eigo Shimizu,[5] Koji Jimbo,[1] Seiko Kato,[1] Takaaki Konuma,[1] Kazuaki Yokoyama,[1] Seiya Imoto,[5] Satoshi Takahashi,[6] Yasuhito Nannya[1,3]

[1]Department of Hematology and Oncology, The Institute of Medical Science Research Hospital, The University of Tokyo, Tokyo, Japan

[2]Department of Laboratory Medicine, The Institute of Medical Science, The University of Tokyo, Tokyo, Japan

[3]Division of Hematopoietic Disease Control, The Institute of Medical Science, The University of Tokyo, Tokyo, Japan

[4]Department of Hematology and Oncology, The University of Osaka Graduate School of Medicine, Osaka, Japan

[5]Division of Health Medical Intelligence, Human Genome Center, The Institute of Medical Science, The University of Tokyo, Tokyo, Japan

[6]Division of Clinical Research Platform, The Institute of Medical Science, The University of Tokyo, Tokyo, Japan

***Corresponding author:** Aki Sato

Department of Hematology and Oncology, The Institute of Medical Science Research Hospital, The University of Tokyo

4-6-1 Shirokanedai, Minato-ku, Tokyo 108-8639, Japan

Phone: +81-3-5449-5542

Fax: +81-3-5449-5429

E-mail: akisato@ims.u-tokyo.ac.jp

Running title

CH environment-derived IDCT and CMML

Acknowledgments: We thank the patient and her family, as well as Dr. Seiya Imoto for organizing the analysis of clinical sequencing data, hosting the Molecular Tumor Board for clinical sequencing cases, and providing research funding for sequencing costs.

Funding: This study was funded by the Agency for Medical Research and Development (Grant Nos. 24ck0106852h0002 and 24ck0106989h0001), Japanese National Research Group on Idiopathic Bone Marrow Failure Syndromes (Grant No. 23FC1024), Japan Society for the Promotion of Science (Grant No. 23K07852), and Japanese Society of Hematology, Kanto-Koshinetsu district.

Authors' contributions: A.S. contributed to the study design, manuscript drafting, and the data analysis and interpretation. Y.N. conceived the experiments, interpreted data, and supervised the study. N. Y., H. T., E. S., K. Y., and S. I. performed the experiments. All authors interpreted the data,

critically revised the report, commented on drafts of the manuscript, and approved the final version.

Conflict of interest: A.S. received manuscript and lecture fees from Novartis Pharma Co.; K.Y. worked at Liquid Mine Co. and received research funding from Nippon Shinyaku and Liquid Mine Co.; S. Imoto received honoraria from Daiichi Sankyo RD Novaré, BrightPath Biotherapeutics Co. Ltd., and Liquid Mine Co.; and Y.N. received lecture fees from Novartis Pharma Co. Ltd. The remaining authors have no conflicts of interest to declare.

Data sharing statement

Individual participant data will not be shared.

Text word count: 1867 (1500)

Number of figures: 3 (≤ 3)

Number of references: 18 (≤15)

Langerhans cell histiocytosis (LCH), Erdheim-Chester disease (ECD), and indeterminate dendritic cell tumor (IDCT) have been reported to be frequently associated with additional hematopoietic malignancies.[1-3] A retrospective analysis of patients with ECD has shown that those harboring clonal hematopoiesis (CH) are more likely to develop myeloid hematopoietic malignancies.[4] However, the timing of CH acquisition and its impact on the development of additional hematopoietic malignancies remain unclear.[5] Herein, we report that IDCT, chronic myelomonocytic leukemia (CMML), and hematopoietic stem cells (HSCs) share two major drivers, *IDH2* p.R140Q and *RUNX1* p.S167R. Our results indicate that, although IDCT and CMML share common driver mutations, clonal divergence had occurred long before disease onset, as revealed by trajectory analysis based on whole-genome sequencing (WGS). This observation suggests that transdifferentiation is unlikely to be the underlying mechanism and instead supports the association of CH-related mutations, such as *IDH2*, with the development of hematopoietic malignancies, including histiocytic neoplasms.

A 68-year-old woman was referred to our hospital for a cutaneous mass and pain. The mass was initially suspected to be LCH, and thrombocytopenia had persisted for 1 year before the skin lesions appeared. She was under regular follow-up for her diabetes mellitus and showed decreased white blood cell (WBC) and platelet levels 3 years ago (Figure 1A). The patient had anemia just before she visited us, in addition to bleeding and pain from the skin tumor, explaining her poor performance status (PS3). Peripheral blood examination

upon admission to our hospital revealed the following: WBC count, 12.9×10^9/L (neutrophils 48.5%, monocytes 25.5%, eosinophils 1.5%, metamyelocytes 1.5%, myelocytes 1.5%, promyelocytes 0%, blasts 0%); red blood cell count, 2.15×10^{12}/L; hemoglobin, 6.3 g/dL; hematocrit, 20.5%; and platelets, 141×10^9/L (Figure 1B). Skin biopsy performed at diagnosis showed massive mononuclear cell infiltration in the dermis, which was positive for CD1a, S-100, CD1c, and VE1 (*BRAF*^{V600E} mutation-specific antibody), and negative for CD207 (langerin) and CD115 (colony stimulating factor 1 receptor [CSF1R]) (Figure 2A). Based on these findings, we diagnosed her with IDCT. Infiltration of IDCT cells was also observed in the bone marrow (BM) (Figure 2B). Bone marrow (BM)-infiltrating CD1a-positive, CD207-negative cells—such as those observed in IDCT—were positive for CD1c and negative for CD115, supporting their classification as dendritic cell neoplasms rather than monocyte/macrophage-lineage tumors (Figure 2C). Multiple lesions with ^{18}F-fluoro-2-deoxyglucose (FDG) uptake were detected in the bone, skin, and muscle by positron emission tomography/computed tomography (PET/CT). Following two cycles of cyclophosphamide, doxorubicin, vincristine, and prednisolone (CHOP) therapy, the skin mass reduced, and the IDCT cells disappeared from the BM. However, an increase in monocytes in the peripheral blood persisted for 3 months, and marrow examination revealed CMML. We confirmed that the patient fulfilled all the essential criteria and one of the desirable criteria (clonal cytogenetics) with monocyte counts of 1.55×10^9/L (>1.0×10^9/L). Peripheral blood examination at first visit to our hospital revealed a WBC count of 12.9×10^9/L and supported the diagnosis of myelodysplastic CMML diagnosis. After five cycles of CHOP

therapy, complete metabolic remission was confirmed by PET/CT, and normalization of soluble interleukin-2 (sIL-2R) was observed. Considering the poor prognosis of disseminated IDCT and complications caused by CMML, we planned to perform unrelated cord blood transplantation (uCBT). However, 1 month after the sixth CHOP therapy cycle, CMML progressed to acute myeloid leukemia (AML), and the IDCT skin lesions relapsed. Venetoclax and azacitidine reduced AML cells; however, IDCT-related cutaneous masses showed progressive enlargement. To achieve deeper remission of IDCT, we used Dabrafenib 150 mg and Trametinib 1 mg (BRAF/MEK inhibitors) as a bridge therapy to uCBT. There was complete regression of the skin lesion, and the sIL-2R levels normalized after 21 days of the bridge therapy. The *BRAF* ^{V600E} mutation in peripheral blood cell-free DNA (plasma cf*BRAF*^{V600E}) became negative. The patient underwent uCBT after conditioning with TBI (4 Gy), busulfan, fludarabine, and G-CSF-cytarabine. Acute graft-versus-host disease (GVHD) prophylaxis was initiated using cyclosporine A and mycophenolate mofetil. Engraftment was achieved on day 20, and she developed grade III GVHD (skin stage 1, intestine stage 2, liver stage 0), which was successfully treated with prednisolone. Plasma cf*BRAF*^{V600E} levels remained negative after the uCBT. Maintenance therapy with BRAF/MEK inhibitors was resumed on day 62. The patient has chronic GVHD of the skin, which is controllable. However, she was negative for both AML and IDCT on day 300 after uCBT. Figure 1 summarizes the patient's clinical course.

This study was approved by the Ethics Committee of the Institutional Review Board of the Institute of Medical Science, University of Tokyo (approval

numbers: 2021-63-1222 and 2022-12-0616) and was conducted per the principles of the Declaration of Helsinki. Clinical samples were collected after obtaining written informed consent from the patient.

To investigate the clonal relationship between IDCT and CMML, we isolated CD34+ and CD14+ cells from the BM by FACS sorting (Figure 3A) and skin biopsies of the IDCT lesions. We conducted whole-exome sequencing (NextSeq 2000; Illumina, San Diego, CA, USA) using the patient's nail-derived DNA as a germline control. Using the Genomon 2.6.2 pipeline,[6] we identified mutations in (a) *IDH2* p.R140Q with variant allele frequency (VAF) of 33% in skin, 53% in CD14+ BM, and 52% in CD34+ BM, (b) *RUNX1* p.S167R in VAF of 30% in skin, 51% in CD14+ BM, and 51% in CD34+ BM, and (c) *BRAF* p.V600E with VAF of 25% in the skin (Figure 3B). The VAF values for *IDH2* and *RUNX1* mutations in CD34+ BM cells (nearly 50%) indicated that almost all stem/progenitor cells of the hematopoietic system were composed of *IDH2*/*RUNX1*-mutated clones; and the expansion of this clone may explain the thrombocytopenia that preceded IDCT. No CMML-specific myeloid driver mutations were identified. The absence of *BRAF* p.V600E alleles in CD34+ BM was confirmed by targeted sequencing at a depth of 1233, suggesting that skin and BM IDCT originated from differentiated cells. Given that IDCT and CMML were developed within a short period of 12 months and they had *RUNX1/IDH2* mutations in common, we initially assumed that the IDCT and CMML clones had bifurcated recently. We, therefore, examined the trajectories of these clones by WGS of skin (IDCT) and CD14+ BM (CMML) samples. WGS libraries were prepared using a TruSeq Nano DNA Library Prep kit with 100 ng of input

DNA and sequenced on a NovaSeq 6000 platform with 150-base paired-end reads (Illumina; San Diego, CA, USA). After filtering out single nucleotide polymorphisms and error calls, 564 events (524 variant types) were identified from two samples. Contrary to expectations, the two samples shared only 40 mutations, while the remaining 484 (86%) were private mutations (Figure 3C). Next, we estimated the time of the most recent common ancestors (MRCA) appearance of these clones (T(MRCA)) based on the ratio of shared/private variants using the formula below:

$$T(MRCA) = \left[A\frac{c}{c+\frac{p_1}{f}},\ A\frac{c}{c+\frac{p_2}{f}} \right]$$

where A is the age at sampling, c is the number of common mutations, p_1 and p_2 are the number of private mutations, and f represents clone fitness.

Assuming that the rate of mutation acquisition remained constant irrespective of driver mutation acquisition (f=1) and given that the patient was 68 years old at the time of sample collection, the MRCA of these clones was estimated to have existed at the age of 9.3 to 10.1, more than 50 years before the onset of these diseases (Figure 3E). This finding is consistent with the high VAF values of *IDH2*/*RUNX1* mutations in CD1a-/CD34+ cells. If higher clone fitness (f>1) is assumed for the IDCT or CMML clones, T(MRCA) becomes more recent but remains considerably earlier than the disease onset (Figure 3F).

IDCT is a rare histiocytic neoplasm of dendritic cell progenitor origin, which is CD1a positive and langerin negative. Like other histiocytic neoplasms, IDCT has been reported to coexist with other hematologic neoplasms, accounting for 22%–42% of cases.[3,7] The most common hematological malignancies that

coexist with IDCT are lymphoid tumors and CMML.

The exact reasons for the high rate of multiple hematological neoplasms in patients with IDCT remain elusive. However, evidence suggests that the transdifferentiation of lymphoid neoplasms into dendritic cells may be a potential cause. In one reported case, both IDCT and the coexisting chronic lymphocytic leukemia had variable diversity-joining (VDJ) rearrangements of the same clonotype.[8] In another case, diffuse large cell lymphoma and IDCS, an IDCT-related neoplasm, shared MYC translocations.[9] These cases support the role of transdifferentiation between IDCT and coexisting neoplasms, as lymphoid neoplasms exhibit irreversible signs of lymphoid cell differentiation or lymphoid neoplasm development.

In contrast, there is no evidence supporting the role of transdifferentiation in cases of CMML co-occurring with IDCT, although shared mutations are often detected between the two.[10] Compared with lymphoid tumors, proving that IDCT cells originate from cells that were previously differentiated into CMMLs is difficult since myeloid cells do not leave any trace of differentiation in the genome. Instead, given the chronological proximity of onset and the presence of shared driver mutations between IDCT and CMML, we suspected that these tumors were clonally related and examined their genetic relationship using trajectory analysis based on WGS. Our results showed that although IDCT and CMML shared driver mutations, clonal bifurcation occurred long before disease onset, making transdifferentiation an unlikely explanation.

Instead, our results highlighted CH as an underlying environmental factor of both tumors. Specifically, CH harboring the *RUNX1/IDH2* mutation serves as

the source of myeloid neoplasm development. *RUNX1*- and *IDH2*-mutated CH carries a significantly higher risk of myeloid neoplasm development than the overall CH-positive population, with hazard ratios of 14.28- and 13.32-fold for *RUNX1* and *IDH2*, respectively.[11] While CH generally induces an inflammatory environment that confers selective advantage of CH clones,[12] each genetic alterations representing CH have distinct mechanisms: *RUNX1* deficiency is associated with the overproduction of tumor necrosis factor alpha (TNF-α), macrophage inflammatory protein 1α, and interleukin (IL)-1α,[13] and *IDH2* mutation induces hypermethylation phenotype through the overproduction of 2-hydroxyglutarate and functional inhibition of ten-eleven translocation-2.[14] Therefore, *RUNX1*/*IDH2*-mutated CH may have played significant role in the development of these tumors in this case. When CMML and/or IDCT developed, substantial secretion of pro-inflammatory signals (granulocyte–macrophage-colony-stimulating factor, TNF-α, IL-6, IL-17, and IL-1β) was achieved from both CMML[15] and histiocytic neoplasms,[16] which consequently promoted both tumors' proliferation.[16,17] This explains the chronological proximity of the development of these tumors despite the long-standing CH environment.

IDCT is a rare disease, and standard treatment guidelines have not yet been established. In cases of IDCT with coincidental non-histiocytic hematopoietic neoplasms, treatment is administered not for IDCT itself, but for the concomitant tumors that have a greater impact on prognosis. In addition, IDCT with non-histiocytic hematopoietic neoplasms has a significantly poorer prognosis [3,18] and hematopoietic stem cell transplantation (HSCT) is considered whenever available. The pre-HSCT treatment strategy primarily focuses on control of

coincidental non-histiocytic hematopoietic neoplasms. However, in cases of IDCT with a *BRAF* ^{V600E} mutation, combination therapy using BRAF/MEK inhibitors is a less toxic modality for debulking the IDCT burden before HSCT. Specific considerations for CH environment-derived IDCT and coincidental tumors have not yet been established. If SASP- or CH-related inflammatory signals play an important role in tumor development within a CH environment, suppressing these signals may be effective and worth considering.

Although this is only a single case report, the next-generation sequencing and trajectory analysis of the isolated cell fractions are expected to elucidate the mechanism of disease onset and optimize molecular targeted therapy.

References

1.Acosta-Medina AA, Kemps PG, Zondag TCE, et al. BRAF V600E is associated with higher incidence of second cancers in adults with Langerhans cell histiocytosis. Blood. 2023;142(18):1570-1575.

2.Papo M, Diamond EL, Cohen-Aubart F, et al. High prevalence of myeloid neoplasms in adults with non-Langerhans cell histiocytosis. Blood. 2017;130(8):1007-1013.

3.Ozkaya N, Melloul Benizri S, Venkataraman G, et al. Indeterminate DC histiocytosis is distinct from LCH and often associated with other hematopoietic neoplasms. Blood Adv. 2024;8(22):5796-5805.

4.Cohen Aubart F, Roos-Weil D, Armand M, et al. High frequency of clonal hematopoiesis in Erdheim-Chester disease. Blood. 2021;137(4):485-492.

5.Goyal G. CHIPping away at Erdheim-Chester disease. Blood. 2021;137(4):434-436.

6.Nakamura S, Yokoyama K, Shimizu E, et al. Prognostic impact of circulating tumor DNA status post-allogeneic hematopoietic stem cell transplantation in AML and MDS. Blood. 2019;133(25):2682-2695.

7.Horna P, Shao H, Idrees A, Glass LF, Torres-Cabala CA. Indeterminate dendritic cell neoplasm of the skin: A 2-case report and review of the literature. J Cutan Pathol. 2017;44(11):958-963.

8.Hassan F, Zhang H, Idiaquez DW, Pakasticali N, Hyjek E, Hussaini M. KRAS may facilitate transformation of chronic lymphocytic leukemia to histiocytic sarcoma with indeterminate dendritic cell features. Am J Clin Pathol. 2025;164(2):157-162.

9.Ochi Y, Hiramoto N, Yoshizato T, et al. Clonally related diffuse large B-cell lymphoma and interdigitating dendritic cell sarcoma sharing. Haematologica. 2018;103(11):e553-e556.

10. Ellis A, Elbaz Younes I, Shao H, Zhang X. Blastic Indeterminate Dendritic Cell Tumor Associated With Chronic Myelomonocytic Leukemia. Am J Dermatopathol. 2022;44(9):691-695.

11. Weeks LD, Niroula A, Neuberg D, et al. Prediction of risk for myeloid malignancy in clonal hematopoiesis. NEJM Evid. 2023;2(5):10.1056/evidoa2200310.

12. Nathan DI, Dougherty M, Bhatta M, Mascarenhas J, Marcellino BK. Clonal hematopoiesis and inflammation: A review of mechanisms and clinical implications. Crit Rev Oncol Hematol. 2023;192:104187.

13. Bellissimo DC, Chen CH, Zhu Q, et al. Runx1 negatively regulates inflammatory cytokine production by neutrophils in response to Toll-like receptor signaling. Blood Adv. 2020;4(6):1145-1158.

14. Figueroa ME, Abdel-Wahab O, Lu C, et al. Leukemic IDH1 and IDH2 mutations result in a hypermethylation phenotype, disrupt TET2 function, and impair hematopoietic differentiation. Cancer Cell. 2010;18(6):553-567.

15. Franzini A, Pomicter AD, Yan D, et al. The transcriptome of CMML monocytes is highly inflammatory and reflects leukemia-specific and age-related alterations. Blood Adv. 2019;3(20):2949-2961.

16. Bigenwald C, Le Berichel J, Wilk CM, et al. BRAF V600E-induced senescence drives Langerhans cell histiocytosis pathophysiology. Nat Med. 2021;27(5):851-861.

17. Kanagal-Shamanna R, Beck DB, Calvo KR. Clonal Hematopoiesis, Inflammation, and Hematologic Malignancy. Annu Rev Pathol. 2024;19:479-506.

18. Bai L, Kang J, Lian J, et al. Outcomes of cutaneous indeterminate dendritic cell tumors: case report and pooled analysis. Int J Clin Exp Med. 2018;11(10):10820-10824.

Figure legends

Figure 1. Clinical course of the patient.

(A) Longitudinal changes in blood cell counts prior to IDCT diagnosis. Dashed lines indicate the reference ranges over time for each parameter: black for WBC, red for hemoglobin (Hb), and blue for platelets. (B) Clinical course and treatment; skin tumor of IDCT; axial images from combined PET/CT with ^{18}F-fluorodeoxyglucose (FDG) before treatment, after 5 cycles of CHOP therapy, before Ven/AZA therapy, and before BRAF/MEK therapy; trends in serum sIL-2R (U/mL), VAF of *BRAF* ^{V600E} in peripheral blood cfDNA; and trend in peripheral blood cell counts and BMA findings at time point defined by months since the initial consultation.

IDCT, indeterminate dendritic cell tumor; CMML, chronic myelomonocytic leukemia; AML, acute myeloblastic leukemia; CHOP, CHOP therapy, comprising doxorubicin, vincristine, cyclophosphamide, and prednisolone; Ven/AZA, Ven/AZA therapy, comprising venetoclax and azacitidine; BRAF/MEK therapy, BRAF inhibitor (Dabrafenib) and MEK inhibitor (Trametinib) combination therapy; uCBT, unrelated cord blood transplantation; PET/CT, positron emission tomography/computed tomography; cfDNA (*BRAF* ^{V600E}), *BRAF* ^{V600E} mutation in plasma cell-free DNA; VAF, variant allele frequency; PB, peripheral blood; BMA, bone marrow aspiration; Hb, hemoglobin; PLT, platelets; Neu, neutrophils; Mo, monocytes; Eo, eosinophils; NCC, nucleated cell count; MgK, megakaryocytes; MYBL, myeloblasts; IDCT, indeterminate dendritic cell tumor.

Figure 2. Tumor histological image

Histological images of tumors were created using NDP. View 2 (Hamamatsu Photonics, Shizuoka, Japan). (A) H&E staining of the IDCT in the skin tumor. Low magnification: scale bar = 1 mm. High magnification: scale bar, 25 μm. Immunohistochemical analysis of CD1a, CD207 (Langerin), S100, VE1, CD1c, and CD115 (CSF1R). Scar bar, 1 mm. (B) Wright-Giemsa-stained bone marrow smears at diagnosis. Arrow: IDCT cell. (C) H&E staining of bone marrow clot sections and immunohistochemical analysis of CD1a, CD207 (Langerin), S100, CD34, VE1, CD1c, and CD115 (CSF1R) in the same samples. Scar bar, 100 μm.

IDCT: indeterminate dendritic cell tumor; H&E, hematoxylin and eosin; VE1, *BRAF*^{V600E} mutation-specific antibody; CSF1R, colony stimulating factor 1 receptor.

Figure 3. Genetic analysis of IDCT, CMML, and hematopoietic progenitor cells.

(A) Fluorescence-activated cell sorting (FACS) of bone marrow samples after two cycles of CHOP therapy. Cell sorting of CMML cells (P1), gating on CD14 positive and CD1a negative, and hematopoietic progenitor cells (P2), gating on CD34 positive. (B) VAFs of driver mutations detected by whole-exome sequencing of the sorted fractions of bone marrow cells and skin samples. (C) Clonal evolution inferred from whole exome sequencing. The dotted box indicates bone marrow cells. (D) Waterfall plots showing the somatic mutations detected by whole genome sequencing from the CD1a+ fraction of skin and

CD14+ fraction of bone marrow cells. The y-axis shows the size (VAF) of mutations. Blue colors indicate shared mutations, and private mutations of CD1a+ and CD14+ cells are shown in green and purple, respectively. (E) Estimation of the time of separation of the CMML (CD14+ fraction) and IDCT (CD1a+ fraction) clones. Length of branches represents the number of mutations. (F) Estimation of time when MRCA existed: where A is the age at sampling, c is the number of common mutations, p1 and p2 are the number of private mutations, and f is clone fitness. The estimated time of MRCA existence, T(MRCA), is given by the following equation.

$$T(MRCA) = \left[A\frac{c}{c+\frac{p_1}{f}}, \quad A\frac{c}{c+\frac{p_2}{f}} \right]$$

Gray ribbon indicates the range of estimated time when MRCA existed for the clone fitness values shown on the x-axis.

SSC, side scatter; FSC, forward scatter; VAF, variant allele frequency; CMML, chronic myelomonocytic leukemia; IDCT, indeterminate dendritic cell tumor; BM, bone marrow; MRCA, most recent common ancestor.

Figure 1.

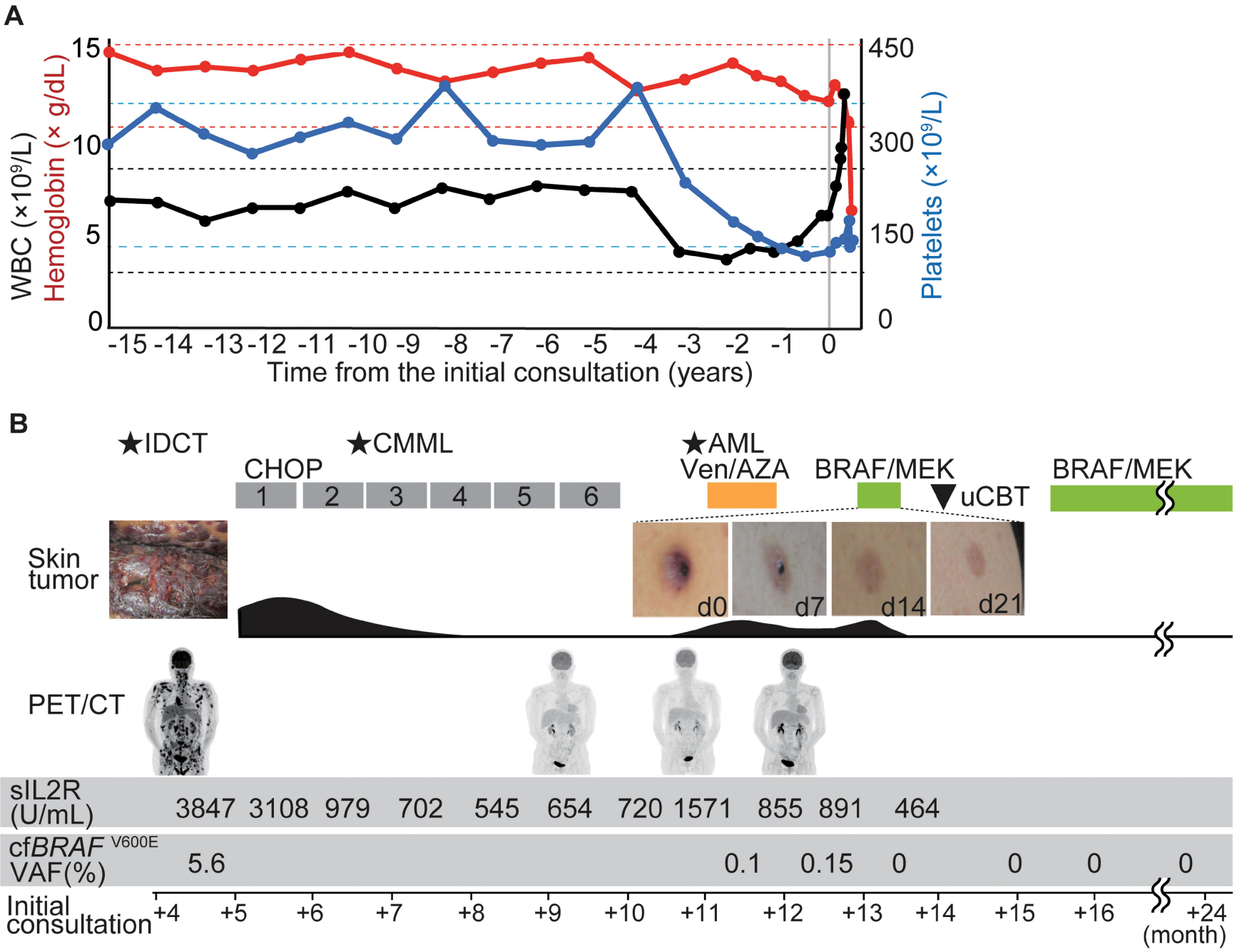

	Months from initial consultation					
PB	+5	+6	+8	+11	+13	+15
WBC (10^9/L)	12.9	4.4	4.2	2.0	3.3	6.1
Hb (g/dL)	6.3	9.4	9.1	11.2	10.6	10.0
PLT (10^9/L)	141	62	202	47	36	47
Neu (%)	48.5	28.5	63.5	29.0	63.0	2.3
Mo (%)	25.5	35.0	16.0	9.0	2.0	6.6
Eo (%)	1.5	0.0	0.0	3.5	1.5	2.5
Blasts (%)	0.0	0.0	0.0	9.0	5.0	0.0

	Months from initial consultation					
BMA	+5	+6	+8	+11	+13	+15
NCC (10^9/L)	221	213	95	162	44	61
MgK (/μL)	30	90	20	30	0	10
MYBL (%)	2.6	0.6	2.2	21.4	10.0	0.9
Mo (%)	14.8	23.9	14.8	4.2	10.2	2.3
Eo (%)	0.0	0.6	0.4	1.0	0.4	6.6
IDCT (%)	8.8	0.0	0.0	0.0	0.0	0.0
Karyotype	46,XX,t(9;14)(q21;q32)					46,XX

Figure 2.

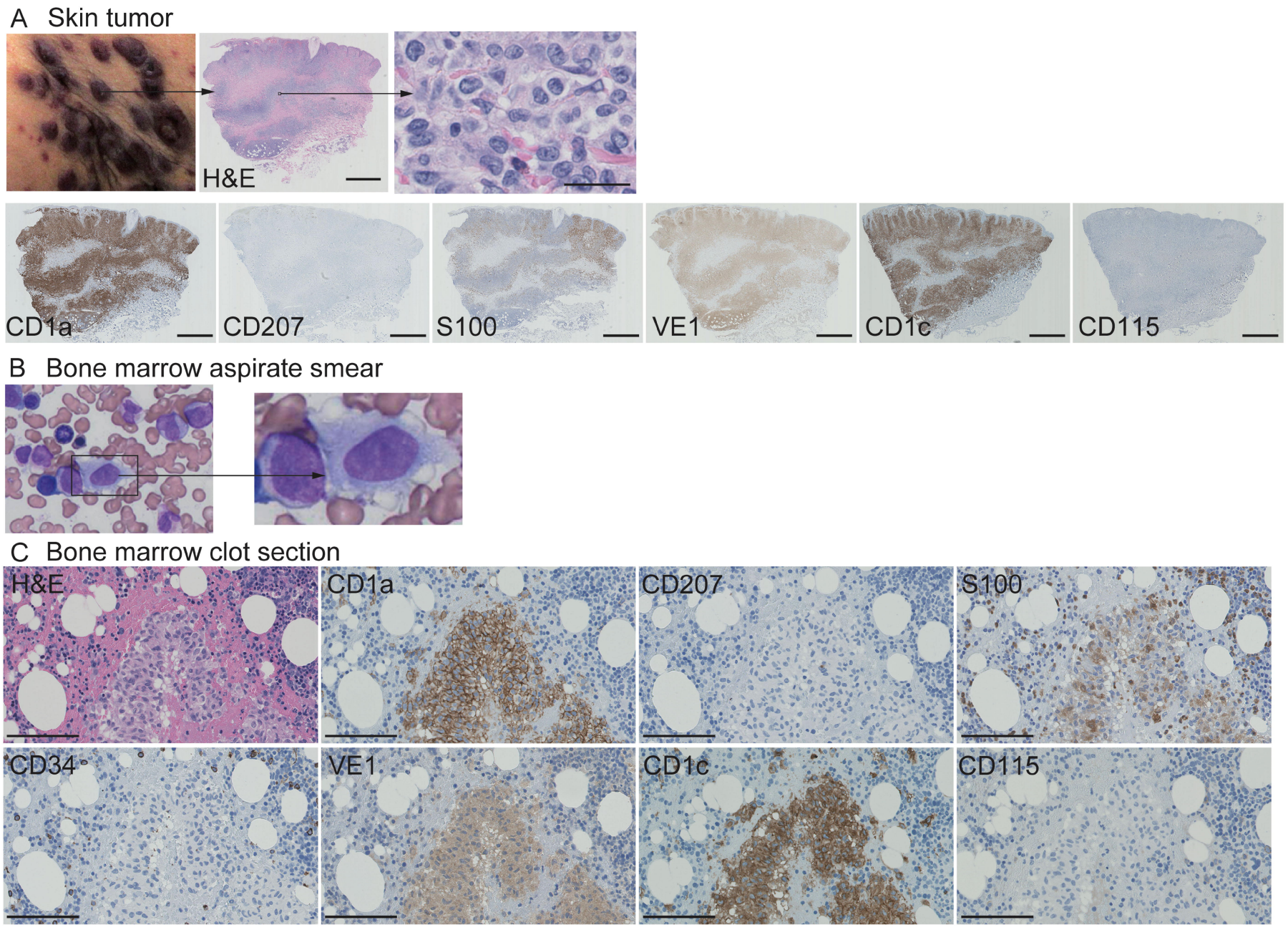
A Skin tumor
H&E
CD1a
CD207
S100
VE1
CD1c
CD115
B Bone marrow aspirate smear
C Bone marrow clot section
H&E
CD1a
CD207
S100
CD34
VE1
CD1c
CD115

Figure 3.

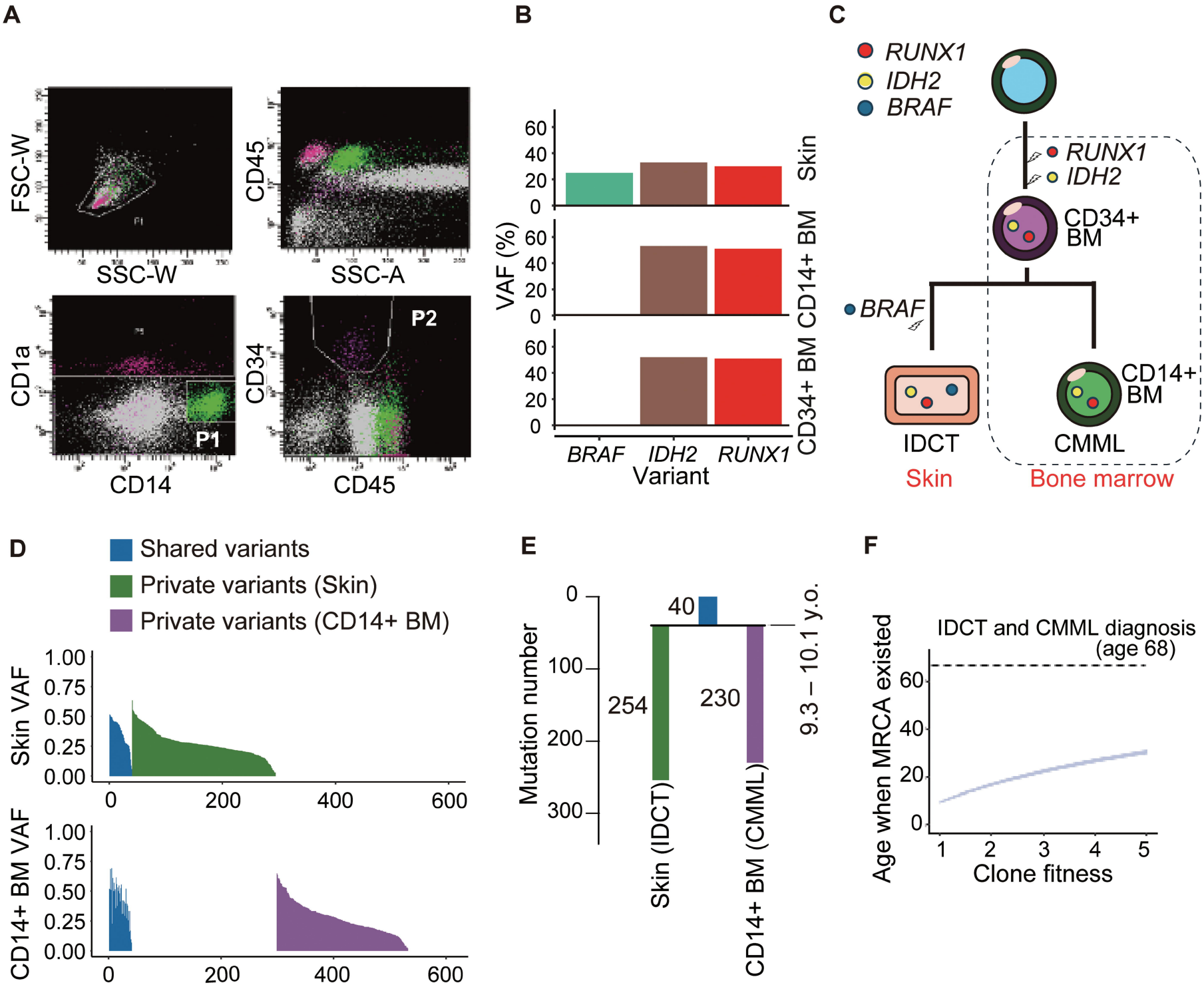
A
FSC-W
SSC-W
CD45
SSC-A
CD1a
CD14
P1
CD34
CD45
P2
B
VAF (%)
60
40
20
0
Skin
CD14+ BM
CD34+ BM
BRAF
IDH2
RUNX1
Variant
C
RUNX1
IDH2
BRAF
CD34+ BM
RUNX1
IDH2
BRAF
CD14+ BM
IDCT
CMML
Skin
Bone marrow
D
Shared variants
Private variants (Skin)
Private variants (CD14+ BM)
Skin VAF
CD14+ BM VAF
1.00
0.75
0.50
0.25
0.00
0
200
400
600
E
Mutation number
0
100
200
300
40
254
230
Skin (IDCT)
CD14+ BM (CMML)
9.3 – 10.1 y.o.
F
IDCT and CMML diagnosis
(age 68)
Age when MRCA existed
60
40
20
0
1
2
3
4
5
Clone fitness